Dislocation contribution to acoustic nonlinearity: The effect of orientation-dependent line energy

W. D. Cash[a] and W. Cai
Department of Mechanical Engineering, Stanford University, Stanford, California 94305-4040, USA

(Received 17 June 2010; accepted 22 November 2010; published online 13 January 2011)

Dislocation dynamics (DD) simulations are used to investigate the acoustic nonlinearity created by dislocations in crystals. The acoustic nonlinearity parameter, β, is quantitatively predicted for a single dislocation bowing in its glide plane between pinning points under a quasistatic loading assumption using DD simulations. The existing model using a constant line energy assumption fails to capture the correct behavior of β for edge dislocations in materials with a nonzero Poisson's ratio. A strong dependence of β on the orientation of Burgers vector relative to the line direction of the dislocation is shown by the DD simulations. A new model using an orientation-dependent line energy is derived for the cases of initially pure edge and screw dislocations. The model is shown to agree with the DD simulations over a range of Poisson's ratio and static stresses. © *2011 American Institute of Physics*. [doi:10.1063/1.3530736]

I. BACKGROUND

Nonlinear ultrasonics is a technique that can be potentially used to nondestructively monitor plastic deformation or fatigue damage in metallic crystals.[1,2] An initially sinusoidal ultrasonic wave is passed through the material and the magnitude of the second harmonic response is measured. The results are commonly expressed in terms of the acoustic nonlinearity parameter, β, which can be defined in terms of experimentally measurable quantities as

$$\beta^{\text{meas}} = \frac{8A_1}{k^2 A_2^2 x}, \tag{1}$$

where k is the wave number, x is the propagation distance of the ultrasound, and A_1 and A_2 are the measured displacement amplitudes of the first and second harmonics, respectively. The importance of β can be easily illustrated in the one-dimensional nonlinear wave equation:

$$\frac{\partial^2 u}{\partial t^2} = c^2\left(1 - \beta\frac{\partial u}{\partial x}\right)\frac{\partial^2 u}{\partial x^2}, \tag{2}$$

where c is the infinitesimal-amplitude wave speed and $\partial u/\partial x$ is the displacement gradient. When β is zero, the equation reduces to the linear wave equation.

Originally, nonlinear ultrasonics was used to study materials that have been subjected to uniaxial loading[1] but over the past two decades a significant interest in using nonlinear ultrasonics to detect fatigue damage has arisen. β is found to grow in magnitude with the number of load cycles until failure in single and polycrystalline metals and alloys.[2,3] Thus, nonlinear ultrasonics has the potential to monitor the entire fatigue life. This is a significant improvement over traditional techniques that rely on the detection of macrocracks.[4] Unfortunately, the underlying mechanisms giving rise to the increase in β are not well understood. The anharmonicity of the crystal itself leads to nonlinearities but for the range of deformations considered its contribution to β essentially remain constant.[1] As a material deforms plastically under uniaxial or cyclic loading there are microstructural changes associated with the growth and patterning of dislocations. The interaction of the ultrasonic waves with the dislocations is thought to be the cause of the variation in β. Proposed analytical models include a dislocation segment bowing between pinning points in its glide plane and the oscillation of two dislocations in a dipole.[3,5] These two dislocation effects have served as the foundation of more advanced models.[6–8] However, the relative weights of these effects have not been conclusively determined. There has yet to be any direct comparison of β calculated using these models to experiments, because of the complexity of real dislocation structures. Not understanding the mechanisms makes it impossible to quantitatively predict β or how a given value of β relates to the damage in the material. Dislocation dynamics (DD) simulations are already being used to study the dislocation microstructure evolution in uniaxial and cyclic loading conditions[9,10] but DD have yet to be applied to the acoustic nonlinearity. Thus, the goal of this paper is to use DD simulations to examine the analytical models and establish DD as a method to predict the contribution of dislocations to β.

II. SIMULATION DESIGN

The DD simulations were performed using a quasistatic loading assumption, as opposed to modeling the dynamic wave propagation. A series of simulations were performed for a given dislocation structure over a range of static external stresses. The structure was allowed to reach equilibrium and the strain due to dislocation motion was calculated. A relationship between stress and dislocation strain was then derived. The deviation of this relationship from linearity is measured by β, as explained later in this paper. The quasistatic loading assumption has been used in previous analytical models and greatly reduces the complexity of the simulations.[5] It is valid because inertial forces on dislocations can be ignored for the loading frequency applied by

[a]Electronic mail: wcash@stanford.edu.

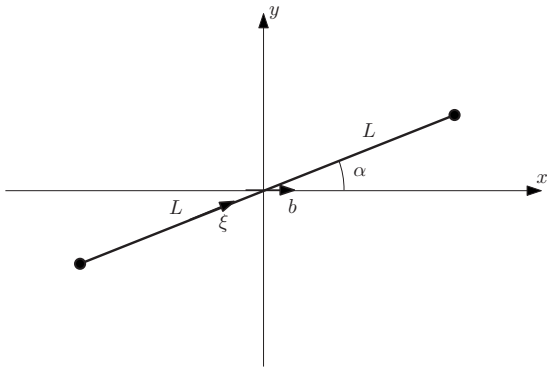

FIG. 1. Schematic of model design. Initially straight dislocation segment of length $2L$ in the x-y plane with a Burgers vector b along the x-axis. The dislocation is oriented along the line direction ξ at an angle α relative to the x-axis.

ultrasonic transducers (0.1–100 MHz) and the small stresses applied by the transducer essentially result in a perturbation about a given stress on the quasistatic stress-strain relationship.

To be consistent with the notation used by DeWit and Koehler,[11] all the simulations performed in this paper are of a single straight dislocation in the x-y plane with initial length $2L$. Its Burgers vector b is along the x-axis and its line direction ξ is oriented at an angle θ relative to b, as shown Fig. 1. An application of a resolved shear stress results in a local radius of curvature r.

The simulations were performed using the PARADIS code.[12] These simulations are limited to the bulk of an fcc single crystal oriented for single slip and the dislocations are initialized as perfect dislocations. The model assumes that cross-slip and thermally activated climb do not occur, because of the small stresses applied by the ultrasound transducers and short time scales present in physical experiments. The dislocation interactions will be modeled throughout this paper using either a line-tension model or using elastic interactions.[12,13] For the case of the elastic interactions, the dislocation will be treated as a long, straight dislocation pinned along the majority of its length, as shown in Fig. 2, to avoid terminating the dislocation inside the crystal and to include the interaction forces of remote segments. Additional simulation parameters are provided in subsequent sections for individual cases.

III. CONSTANT LINE TENSION MODEL OF HIKATA *ET AL.*

A. Model construction

The model developed by Hikata *et al.* was the first to employ the quasistatic loading assumption for the bowing dislocation line.[5] For the past four decades, it has been the widely accepted model for the acoustic nonlinearity arising from the self-interaction of a single dislocation. Only a brief description of this model is given here; the reader is referred to the detailed derivation given by Cantrell.[14] However, a trivial deviation from previous derivations has been made here to consider a shear wave passing though the material as opposed to a longitudinal wave; this only simplifies the notation.

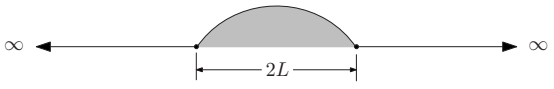

FIG. 2. Infinitely long, straight dislocation pinned along majority of its length modeled by the elastic interaction DD simulations.

A line-tension approximation is used to represent the shape of the dislocation bowing between pinning points under an applied stress σ. The line-tension T is assumed to be constant regardless of orientation, $T=\mu b^2/2$. Therefore, screw and edge dislocations possess the same line energy, and the equilibrium shape is that of a circular arc with a constant radius of curvature. The area swept by the dislocation can be expanded in a series approximation to yield an expression for dislocation strain in terms of powers of applied stress σ

$$\epsilon^{\mathrm{dis}} = \frac{2}{3}\frac{\Omega\Lambda^{\mathrm{dis}}L^2R^3}{\mu}\sigma + \frac{4}{5}\frac{\Omega\Lambda^{\mathrm{dis}}L^4R^3}{\mu^3 b^2}\sigma^3, \tag{3}$$

where Λ^{dis} is the dislocation density, μ is the shear modulus, R is an orientation factor between the applied stress and the resolved shear stress, and Ω is conversion factor between shear strain in the slip direction and measured strain.

The elastic strains of the lattice can also be expressed as a series in terms of σ

$$\epsilon^{\mathrm{lat}} = \frac{\partial u_1}{\partial x_2} = \frac{1}{A_{66}}\sigma - \frac{1}{2}\frac{A_{666}}{A_{66}^3}\sigma^2, \tag{4}$$

where A_{66} and A_{666} are the second and third-order elastic stiffnesses in Voigt notation, respectively. In an elastically isotropic material A_{66} is simply the shear modulus μ. The total strain[15] ϵ is thus the summation of the elastic lattice strain, ϵ^{lat}, and the strain caused by the dislocation, ϵ^{dis}

$$\epsilon = \epsilon^{\mathrm{lat}} + \epsilon^{\mathrm{dis}} = \left(\frac{1}{\mu} + \frac{2}{3}\frac{\Omega\Lambda^{\mathrm{dis}}L^2R^3}{\mu}\right)\sigma - \frac{1}{2}\frac{A_{666}}{\mu^3}\sigma^2 + \frac{4}{5}\frac{\Omega\Lambda^{\mathrm{dis}}L^4R^3}{\mu^3 b^2}\sigma^3, \tag{5}$$

where A_{66} has been replaced with μ. The ultrasonic wave creates a small oscillatory stress of amplitude $\Delta\sigma$ in addition to the static stress σ, which in turn causes an additional strain $\Delta\epsilon$. This can be represented as

$$\Delta\sigma = \frac{\partial\sigma}{\partial\epsilon}\Delta\epsilon + \frac{1}{2}\frac{\partial^2\sigma}{\partial\epsilon^2}(\Delta\epsilon)^2 + \cdots = \left(\frac{\partial\epsilon}{\partial\sigma}\right)^{-1}\Delta\epsilon - \frac{1}{2}\frac{\partial^2\epsilon}{\partial\sigma^2}\left(\frac{\partial\epsilon}{\partial\sigma}\right)^{-3}(\Delta\epsilon)^2 + \cdots, \tag{6}$$

where the derivatives of ϵ can be derived from Eq. (5). It can be shown from Eq. (6) that the total acoustic nonlinearity parameter β^{total} is

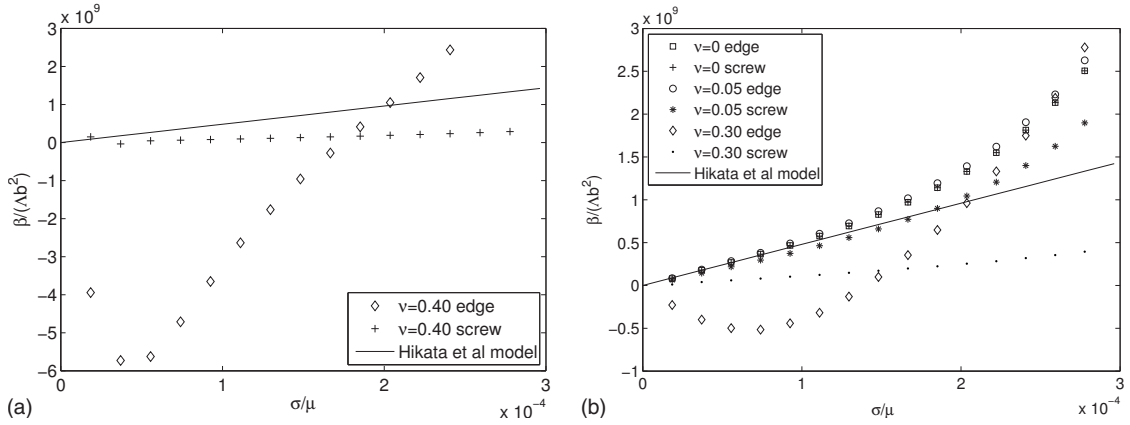

FIG. 3. Comparison of DD simulations with the model of Hikata *et al.*

$$\beta^{\text{total}} = \frac{\partial^2 \epsilon}{\partial \sigma^2}\left(\frac{\partial \epsilon}{\partial \sigma}\right)^{-2} = \left(-\frac{A_{666}}{\mu^3} + \frac{24}{5}\frac{\Omega \Lambda^{\text{dis}} L^4 R^3}{\mu^3 b^2}\sigma\right) \times \left(\frac{1}{\mu} + \frac{2}{3}\frac{\Omega \Lambda^{\text{dis}} L^2 R^3}{\mu}\right)^{-2}. \tag{7}$$

In most cases

$$\frac{2}{3}\frac{\Omega \Lambda^{\text{dis}} L^2 R^3}{\mu} \ll \frac{1}{\mu}. \tag{8}$$

β^{total} can then be simplified to

$$\beta^{\text{total}} = -\frac{A_{666}}{\mu} + \frac{24}{5}\frac{\Omega \Lambda^{\text{dis}} L^4 R^3}{\mu b^2}\sigma, \tag{9}$$

where A_{666}/μ is the lattice contribution, which is essentially invariant over the range of interest and will henceforth be omitted. The contribution of dislocation monopoles to the acoustic nonlinearity, β^{dis}, can then be expressed nondimensionally as

$$\beta^{\text{dis}} = \frac{24 \Omega R^3}{5}(\Lambda^{\text{dis}} b^2)\left(\frac{L}{b}\right)^4\left(\frac{\sigma}{\mu}\right), \tag{10}$$

where $\Lambda^{\text{dis}} b^2$, L/b, and σ/μ correspond to nondimensional dislocation density, length, and stress, respectively.

B. Comparison with elastic interaction DD simulations

If the applied stress is chosen to act directly on the slip system of the dislocation and the strain is measured relative to the slip direction, Ω and R will both be unity. For this special case, Eq. (10) can be expressed as

$$\frac{\beta^{\text{dis}}}{(\Lambda^{\text{dis}} b^2)} = \frac{24}{5}\left(\frac{L}{b}\right)^4\left(\frac{\sigma}{\mu}\right), \tag{11}$$

where β^{dis} has been divided by the nondimensional density in the material.[16] The analytical model can now be compared with an elastic interaction DD simulation of a pinned dislocation of nondimensional length, L/b, of 1000 between two pinning points. The Poisson's ratio, ν, is chosen to be 0.40, a reasonable value for engineering metals.

The first equality in Eq. (7) shows that β^{dis} can be calculated from DD by taking the first and second derivatives of the dislocation strain with respect to stress about the equilibrium stress σ

$$\beta^{\text{dis}} = \frac{\partial^2 \epsilon^{\text{dis}}}{\partial \sigma^2}\left(\frac{\partial \epsilon}{\partial \sigma}\right)^{-2} = \frac{\partial^2 \epsilon^{\text{dis}}}{\partial \sigma^2}\left(\frac{1}{A_{66}} + \frac{\partial \epsilon^{\text{dis}}}{\partial \sigma}\right)^{-2} \approx \mu^2 \frac{\partial^2 \epsilon^{\text{dis}}}{\partial \sigma^2}, \tag{12}$$

where again, the dislocation contribution $\partial \epsilon^{\text{dis}}/\partial \sigma$ to $\partial \epsilon/\partial \sigma$ is minuscule.[17] Therefore, a series of constant-stress simulations were performed to determine the equilibrium dislocation strain ϵ^{dis}. $\partial^2 \epsilon^{\text{dis}}/\partial \sigma^2$ was then found using a central difference scheme.

The results in Fig. 3(a) highlight the disagreement between the Hikata *et al.* model and the DD simulations using the PARADIS program.[12] The deviation from the linear relationship of β^{dis} and σ predicted by the model is most dramatic for the edge dislocation with a negative β^{dis} at small stresses.

C. Comparison with line energy DD simulations

In order to simplify the DD simulations and better evaluate the analytical model, a series of simulations using an orientation-dependent line energy model were performed.[13] A comparison of these simulations and the analytical results are shown in Fig. 3(b) for pure edge and screw monopoles over a range of Poisson's ratios ν and σ.[18] When σ is small, the results agree well for both screw and edge if ν is close to zero. When ν is small, screw and edge dislocation have approximately the same line energies and their behavior should be adequately captured by the constant line-tension model used by Hikata. However, when ν is increased the line energy DD predictions deviate from the Hikata model, with that of the edge taking on a wildly different shape for ν greater than approximately 0.2. Unfortunately, most engineering metals and alloys possess Poisson's ratios in the range of 0.2–0.4. In materials with a large Poisson's ratio, screw and edge dislocations have vastly different line energies and the assumption that the dislocation bows out in a circular arc (as predicted by the Hikata model) may no longer be valid. These results indicate that the orientation-dependence of the line energy may significantly affect the

acoustic nonlinearity. It is thus desired to develop an analytical model to examine whether the orientation-dependence of the line energy is indeed responsible for the discrepancies observed here.

IV. VARIABLE LINE-ENERGY MODEL

The previous section suggests that assuming the dislocation line energy to be constant may be an oversimplification with serious consequences. The major difficultly that arises when moving to a variable line-tension is that the shape of the bowed dislocation can no longer be described by a simple circular arc with constant radius of curvature. The equilibrium shape of a bowing monopole under an arbitrary load was solved by DeWit and Koehler by balancing the work done by the external stress and the change in the self-energy of the dislocation.[11] The equilibrium shape of a dislocation loop under an external stress τ with Burgers vector b along the x-axis can be parameterized in terms of the local line orientation θ

$$x = \frac{1}{\tau b}\left[E(\theta)\sin\,\theta + \frac{dE}{d\theta}\cos\,\theta\right], \tag{13}$$

$$y = \frac{1}{\tau b}\left[E(\theta)\cos\,\theta - \frac{dE}{d\theta}\sin\,\theta\right] \quad \theta \in [0,2\pi]. \tag{14}$$

The orientation-dependent line energy $E(\theta)$ is commonly expressed as

$$E(\theta) = \frac{\mu b^2}{4\pi(1-\nu)}(1-\nu\cos^2\,\theta)\ln\left(\frac{r_o}{r_i}\right), \tag{15}$$

in an isotropic elastic medium, where r_o and r_i are the outer and inner cutoff radii, respectively.[19] A numerical implementation of this model is employed in the aforementioned line energy DD simulations.[13] For comparison with the Hikata *et al.* model, $\ln(r_o/r_i)$ is approximated as 2π and we can define

$$M = \frac{\mu b^2 \ln\left(\frac{r_o}{r_i}\right)}{4\pi(1-\nu)} = \frac{\mu b^2}{2(1-\nu)} \tag{16}$$

and rewrite Eq. (15) as

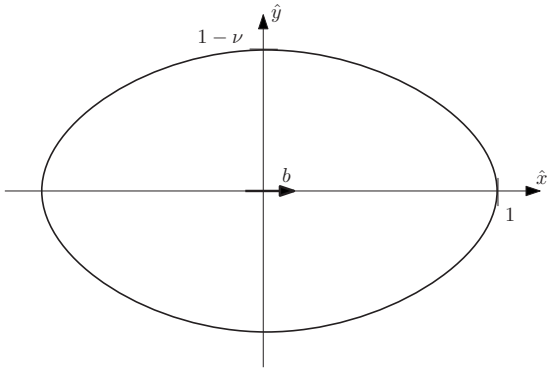

FIG. 4. Equilibrium shape of dislocation loop for ν=0.33 in scaled coordinates.

$$E(\theta) = M(1-\nu\cos^2\,\theta). \tag{17}$$

Thus, in the case of ν=0, Eq. (17) simplifies to the constant line energy, $\mu b^2/2$, as used in the Hikata *et al.* model.

Evaluating Eqs. (13) and (14) with the line energy defined in Eqs. (16) and (17) yields

$$\hat{x} \equiv \frac{\tau b x}{M} = C\,\sin\,\theta + D\,\sin\,3\theta, \tag{18}$$

$$\hat{y} \equiv \frac{\tau b y}{M} = U\,\cos\,\theta + V\,\cos\,3\theta, \tag{19}$$

where

$$C = 1+\frac{\nu}{4}; \quad D = \frac{\nu}{4}; \quad U = 1-\frac{5\nu}{4}; \quad V = \frac{\nu}{4}. \tag{20}$$

This defines the parameterized curve for the generalized equilibrium shape of the dislocation loop, as shown in Fig. 4 for ν=0.33. Although the curve may appear nearly elliptical, any such approximation should be avoided because the errors in the shape of the curve will be amplified in the derivatives of Eq. (7) to find β^{total}. The deviation from ellipticity becomes apparent at Poisson's ratios approaching 0.5. In the case of ν=0, the dislocation loop simplifies to a unit circle in the $\hat{x},\hat{y}$ coordinate system.

The unstable equilibrium shape of any dislocation at activation can be found by passing a line through the origin at an angle α, as shown in Fig. 5(a), where α is the angle between the Burgers vector and the initial line direction. The

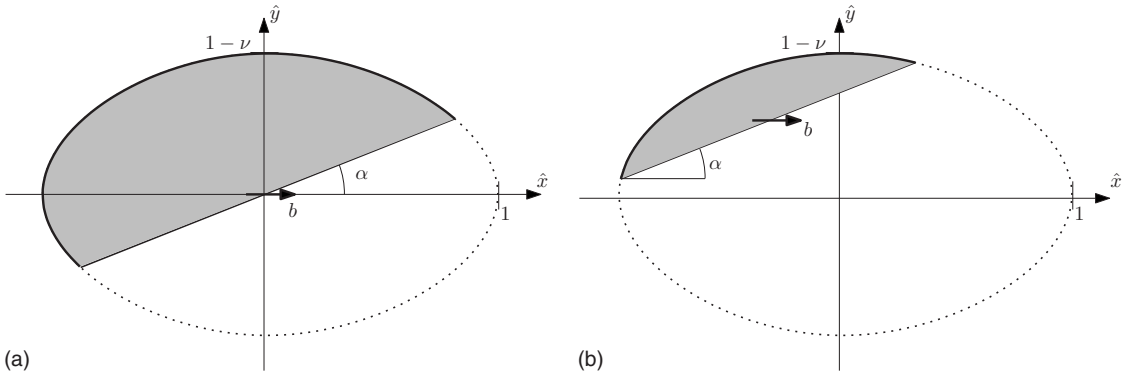

FIG. 5. Curve of an arbitrary pinned dislocation under a resolved shear stress from the equilibrium shape of a dislocation loop using variable line energy.

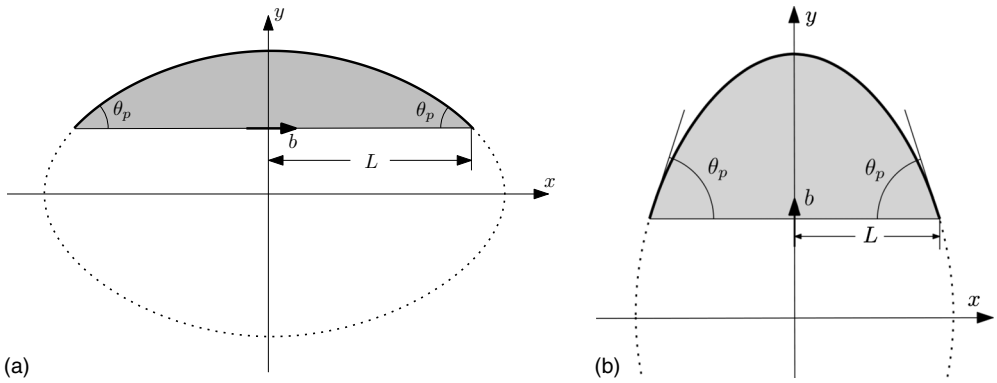

FIG. 6. Shape of pinned dislocations subjected to a resolved shear below the activation stress.

shape of the deformed dislocation prior to activation can be found from the generalized curve by shifting the line along its normal, as shown in Fig. 5(b).

The strain caused by dislocation motion can again be related to the area swept out by the dislocation. The area can be found for an arbitrary dislocation using Eqs. (18) and (19), but for simplicity only initially pure edge and screw dislocations will be considered here. In these special cases, the bowed out shape of the dislocation is symmetric with respect to a plane normal to the initial line direction of the dislocation and passing through its midpoint.

In the case of a screw dislocation, the x-axis is parallel to its initial line direction and the y-axis is along the glide direction. The area swept out by the screw dislocation can be expressed as:

$$A = \int_{-L}^{L} y(x)dx - y(x=L)2L = 2\int_{0}^{L} y(x)dx - y(x=L)2L, \tag{21}$$

where y is now a function of x. Evaluating this expression is not a trivial matter; two different approaches will be taken in the following two sections. The edge dislocation's initial line direction is along the y-direction and the dislocation bows out in the x-direction. To simplify derivations later in this paper, a coordinate transformation is performed so that the edge is initially along the x-direction and glides in the y-direction, as shown in Fig. 6(b). The equation of the dislocation loop in this coordinate system is

$$\hat{x} \equiv \frac{\tau b x}{M} = U\sin\theta - V\sin 3\theta, \tag{22}$$

$$\hat{y} \equiv \frac{\tau b y}{M} = C\cos\theta - D\cos 3\theta. \tag{23}$$

Equation (21) can then be used to find the area swept by the edge dislocation.

V. POWER SERIES SOLUTION

A. Model construction

In this section, the technique used by Hikata *et al.* to express the strains in terms of a power series of stress is applied to the cases of initially edge and screw dislocations with variable line energy defined in the previous section. This eventually leads to an expression of β^{dis} as a power series of stress.

The dislocation curve described in Eqs. (18) and (19) is shifted so that the peak of the curve coincides with the origin. $\hat{y}$ can approximated as a power series of $\hat{x}$

$$\hat{y}(\hat{x}) = \frac{\zeta}{2}\hat{x}^2 + \frac{\eta}{4!}\hat{x}^4 + \frac{\kappa}{6!}\hat{x}^6, \tag{24}$$

where the odd powers of $\hat{x}$ are obviously zero by symmetry and higher order terms are ignored. Expanding Eqs. (18) and (19) for an initially screw dislocation yields

$$\zeta = -\frac{1}{1+\nu}, \tag{25}$$

$$\eta = -\frac{3(1+3\nu)}{(1+\nu)^4}, \tag{26}$$

$$\kappa = -\frac{45(1+6\nu+13\nu^2)}{(1+\nu)^7}. \tag{27}$$

The area in Eq. (21) can be expressed in scaled coordinates as

$$\hat{A} = 2\int_0^{\hat{L}} \hat{y}(\hat{x})d\hat{x} - \hat{y}(\hat{L})\cdot 2\hat{L} = -\frac{2}{3}\zeta\hat{L}^3 - \frac{1}{15}\eta\hat{L}^5 - \frac{1}{420}\kappa\hat{L}^7. \tag{28}$$

To solve for the real area,

$$\hat{L} = \frac{\tau b}{M}L, \tag{29}$$

$$\hat{A} = \left(\frac{\tau b}{M}\right)^2 A, \tag{30}$$

are substituted into Eq. (28) to yield

$$A = -\frac{2}{3}\frac{bL^3\zeta}{M}\tau - \frac{1}{15}\frac{b^3L^5\eta}{M^3}\tau^3 - \frac{1}{420}\frac{b^5L^3\kappa}{M^5}\tau^5. \tag{31}$$

The area swept by the dislocation is directly proportional to the strain of the dislocation,

$$\epsilon^{\mathrm{dis}} = \frac{b\Omega\Lambda^{\mathrm{dis}}}{2L}A = -\frac{1}{3}\frac{b^2L^2\Omega\Lambda^{\mathrm{dis}}\zeta}{M}\tau - \frac{1}{30}\frac{b^4L^4\Omega\Lambda^{\mathrm{dis}}\eta}{M^3}\tau^3 - \frac{1}{840}\frac{b^6L^6\Omega\Lambda^{\mathrm{dis}}\kappa}{M^5}\tau^5, \tag{32}$$

where again Λ^{dis} is the dislocation density. Substituting the values of ζ, η, κ, and M into Eq. (32) and taking $\tau = R\sigma$ as before

$$\epsilon^{\mathrm{dis}} = \frac{2}{3}\frac{(1-\nu)\Omega\Lambda^{\mathrm{dis}}L^2R}{(1+\nu)\mu}\sigma + \frac{4}{5}\frac{(1+3\nu)(1-\nu)^3\Omega\Lambda^{\mathrm{dis}}L^4R^3}{(1+\nu)^4\mu^3b^2}\sigma^3 + \frac{12}{7}\frac{(1+6\nu+13\nu^2)(1-\nu)^5\Omega\Lambda^{\mathrm{dis}}L^6R^5}{(1+\nu)^7\mu^5b^4}\sigma^5. \tag{33}$$

Using derivations similar to that of Hikata *et al.* in Sec. III A, the initially screw dislocation contribution to the acoustic nonlinearity can then be expressed in the following nondimensional form:

$$\frac{\beta_s^{\mathrm{dis}}}{(\Lambda^{\mathrm{dis}}b^2)} = \frac{24(1+3\nu)(1-\nu)^3\Omega R^3}{5(1+\nu)^4}\left(\frac{L}{b}\right)^4\left(\frac{\sigma}{\mu}\right) + \frac{240(1+6\nu+13\nu^2)(1-\nu)^5\Omega R^5}{7(1+\nu)^7b^4}\left(\frac{L}{b}\right)^6\left(\frac{\sigma}{\mu}\right)^3. \tag{34}$$

In the case of $\nu=0$ and the orientation factors R and Ω are unity, Eq. (34) reduces to

$$\left.\frac{\beta_s^{\mathrm{dis}}}{(\Lambda^{\mathrm{dis}}b^2)}\right|_{\nu=0} = \frac{24}{5}\left(\frac{L}{b}\right)^4\left(\frac{\sigma}{\mu}\right) + \frac{240}{7}\left(\frac{L}{b}\right)^6\left(\frac{\sigma}{\mu}\right)^3. \tag{35}$$

The first-order term is identical to Eq. (11) from the Hikata *et al.* derivation. Similar analysis for an initially edge dislocation described by Eqs. (22) and (23) reveals

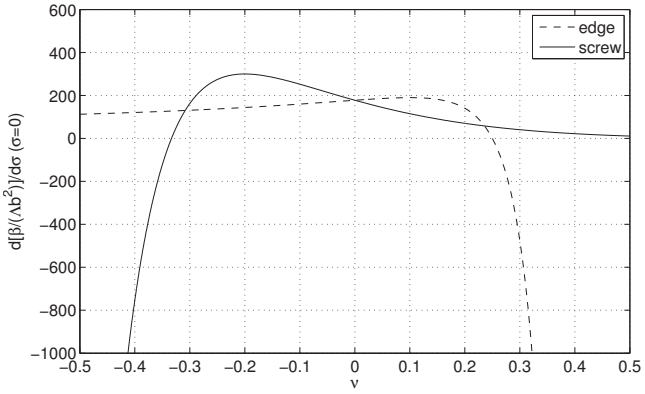

FIG. 7. $\partial\beta/\partial\sigma$ at $\sigma=0$ over a range of Poisson's ratio.

$$\frac{\beta_e^{\mathrm{dis}}}{(\Lambda^{\mathrm{dis}}b^2)} = \frac{24(1-4\nu)(1-\nu)^3\Omega R^3}{5(1-2\nu)^4}\left(\frac{L}{b}\right)^4\left(\frac{\sigma}{\mu}\right) + \frac{240(1-8\nu+20\nu^2)(1-2\nu)^7\Omega R^5}{7(1+\nu)^7}\left(\frac{L}{b}\right)^6\left(\frac{\sigma}{\mu}\right)^3. \tag{36}$$

In order to illustrate the importance of the orientation-dependence of the line energy, the initial slope of the $\beta/(\Lambda^{\mathrm{dis}}b^2)$ as a function of σ is plotted over a range of ν in Fig. 7. The differences between edge and screw dislocations is readily apparent for nonzero Poisson's ratios. Edge dislocations are seen to have initially negative values of β^{dis} for ν greater than 0.25, and tends toward negative infinity as ν approaches 0.5. In screw dislocations the slope is negative for ν less than $-1/3$. However, in subsequent analyses only positive Poisson's ratios will be considered.

B. Comparison with line-tension DD simulations

The newly derived analytical expression for $\beta^{\mathrm{dis}}/(\Lambda^{\mathrm{dis}}b^2)$ was compared with the aforementioned line energy DD simulations, as shown for screw dislocations in Fig. 8(a) and for edge dislocations in Fig. 8(b). It is apparent that the power series solution agrees with the DD simulations significantly better than the Hikata *et al.* model and is able to capture the initially negative β^{dis} exhibited by edge disloca-

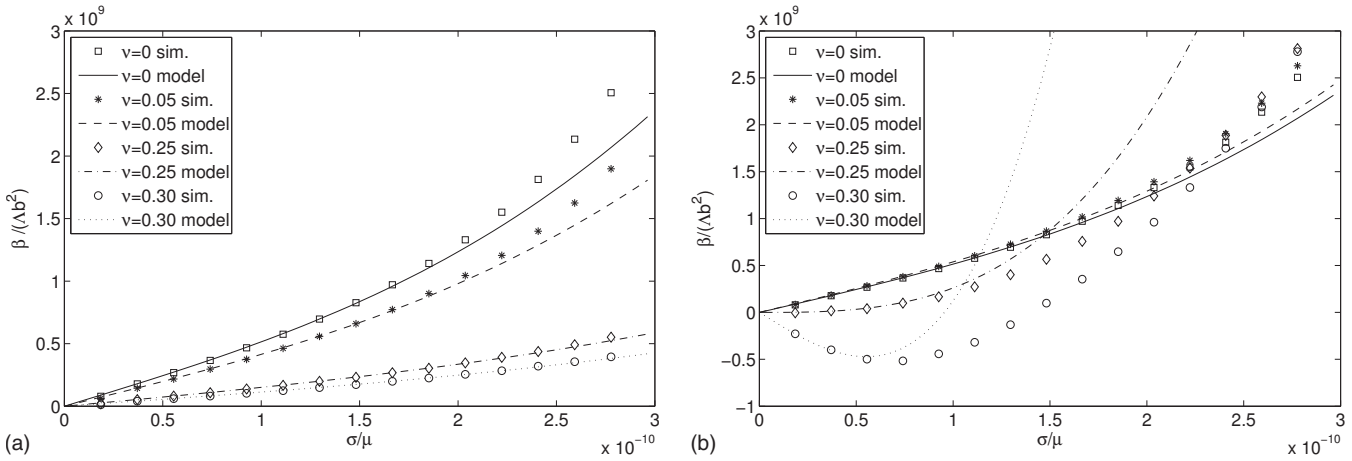

FIG. 8. Comparison of orientation-dependent, line energy DD simulations with the power series model.

tions in materials with large Poisson's ratios. The power series model agrees well for screw dislocations for any ν and for edge dislocations with $\nu < 0.25$. However, for the case of edge dislocations in materials with large ν, the model is only able to roughly predict the general trend at small stresses. This is a consequence of using a truncated power series expanded about zero stress.

VI. IMPLICIT SOLUTION

A. Model construction

In order to avoid the shortcomings of the power series solution at high stress values, the area of the bowed out dislocation in Eq. (21) must be not be approximated. However, this integral cannot immediately be evaluated because x and y are expressed in terms of the parameter θ. Therefore, the area for initially edge or screw dislocations is now expressed in terms of θ as

$$A(\tau, \theta_p) = 2\int_0^{\theta_p} y(\theta)\frac{dx}{d\theta}d\theta - y(\theta = \theta_p)2L, \tag{37}$$

where θ_p is the angle at the pinning point, as shown in Fig. 6(a). This equation is only valid for initially pure edge and screw dislocations, because of their aforementioned symmetry. It addition, it holds true only if $E(\theta) + d^2E(\theta)/d\theta^2 > 0$,[11] because the angle θ must increase monotonically from the midpoint to the pinning point.[20]

Equation (37) expresses A as a function of the applied stress τ and θ_p. But, τ can be expressed as a function of θ_p by evaluating Eq. (18) at $x = L$ and $\theta = \theta_p$ and solving for τ. After substituting $\sigma = R\tau$ the resolved shear stress σ can be expressed as

$$\sigma_s(\theta_p) = \frac{1}{2}, \frac{(1 + \nu\cos^2\theta_p)\sin\theta_p Rb\mu}{L(1-\nu)}, \tag{38}$$

for an initially screw dislocation. In the case of an initially edge dislocation, the same steps can be performed to Eq. (22) to yield

$$\sigma_e(\theta_p) = \frac{1}{2}\frac{(1 - \nu - \nu\cos^2\theta_p)\sin\theta_p Rb\mu}{L(1-\nu)}. \tag{39}$$

Substituting the results of Eqs. (18), (19), and (38) into Eq. (37) gives an expression for A as a function of θ_p for an initially screw dislocation

$$A_s(\theta_p) = \frac{-L^2\left\{\frac{1}{2}\sin 2\theta_p[8\nu^2\cos^4\theta_p - (10\nu^2 - 16\nu)\cos^2\theta_p + (\nu^2 - 24\nu + 8)] + \theta_p(\nu^2 + 8\nu - 8)\right\}}{8R^2\sin^2\theta_p(\nu\cos^2\theta_p + 1)^2}. \tag{40}$$

For an initially edge dislocation, Eqs. (22), (23), and (39) can be substituted into Eq. (37) to yield

$$A_e(\theta_p) = \frac{-L^2\{\sin\theta_p[8\nu^2\cos^5\theta_p + \nu(6\nu - 16)\cos^3\theta_p - (15\nu^2 - 8\nu - 8)\cos\theta_p] + \theta_p(\nu^2 + 8\nu - 8)\}}{8R^2\sin^2\theta_p[\nu^2\cos^4\theta_p + 2\nu(\nu-1)\cos^2\theta_p + \nu^2 - 2\nu + 1]}. \tag{41}$$

The dislocation strain ϵ^{dis} can then be expressed as[21]

$$\epsilon^{\text{dis}}(\theta_p) = \frac{b\Omega\Lambda^{\text{dis}}}{2L}A(\theta_p). \tag{42}$$

Knowing ϵ^{dis} allows β^{dis} to be expressed as

$$\beta^{\text{dis}}(\theta_p) = \frac{\partial^2\epsilon^{\text{dis}}}{\partial\sigma^2}\left(\frac{\partial\epsilon}{\partial\sigma}\right)^{-2}, \tag{43}$$

where ϵ is the total strain. Because ϵ^{dis} is expressed as a function of θ, the derivatives in Eq. (43) must be evaluated as

$$\frac{\partial\epsilon}{\partial\sigma} = \frac{\partial\epsilon^{\text{dis}}}{\partial\sigma} + \frac{1}{\mu} = \frac{\partial\epsilon^{\text{dis}}}{\partial\theta_p}\left(\frac{\partial\sigma}{\partial\theta_p}\right)^{-1} + \frac{1}{\mu}, \tag{44}$$

$$\frac{\partial^2\epsilon^{\text{dis}}}{\partial\sigma^2} = \frac{\partial^2\epsilon^{\text{dis}}}{\partial\theta_p^2}\left(\frac{\partial\sigma}{\partial\theta_p}\right)^{-2}. \tag{45}$$

Substituting the solutions of Eqs. (44) and (45) into Eq. (43) solves for β^{dis} as a function of θ_p.

Thus, an implicit solution for β^{dis} as a function of applied stress σ can be formed by Eq. (38) or Eq. (39) and Eq. (43) in terms of the parameter θ_p for initially screw or edge dislocations, respectively.

B. Comparison with simulations

As expected, the implicit solution exactly agrees with the orientation-dependent line energy DD simulations to within the error introduced by the discretization of the dislocation (not shown). However, special consideration is required to accurately compare the implicit solution with fully elastic DD simulations. The tension factor M of the variable line energy must be scaled, because the exact value of $\ln(r_o/r_i)$ is unknown for an arbitrary dislocation shape. Thus, the assumption that $\ln(r_o/r_i)$ is simply 2π is no longer used. The elastic DD results cannot be simply scaled to match the implicit model because the solution of Eq. (43) has a nontrivial dependence on M. Thus, Eq. (16) can be rewritten as

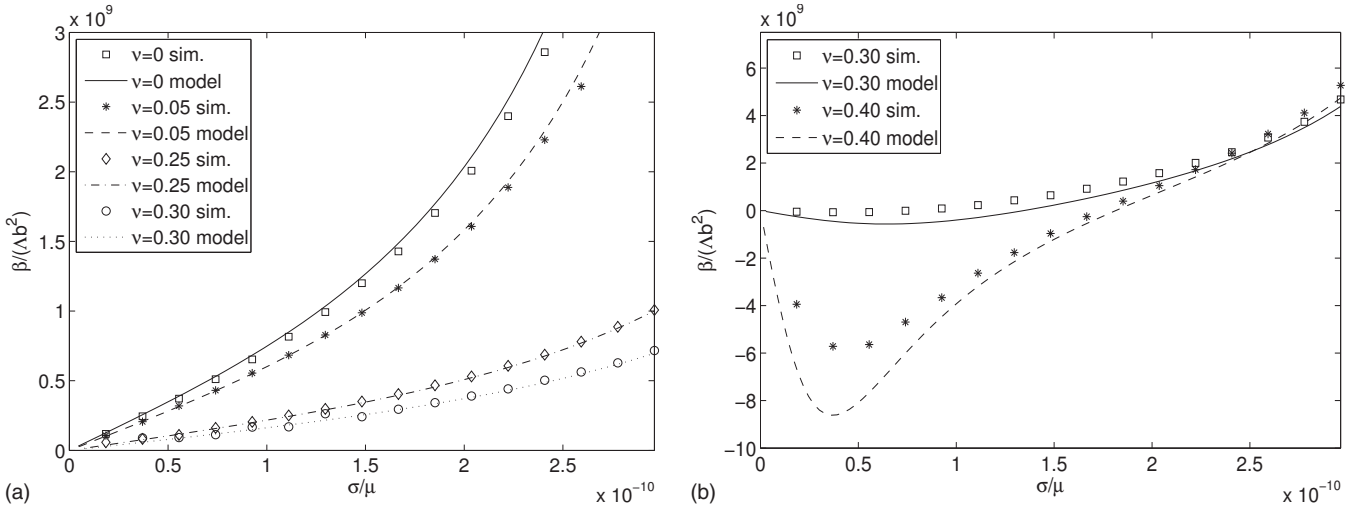

FIG. 9. Comparison of elastic interaction DD simulations with the implicit model.

$$M = \frac{\mu b^2}{4\pi(1-\nu)} t, \tag{46}$$

where t is scale factor that is found by fitting the activation stress of the line-tension model with that of the elastic interaction DD simulation for a single value of ν. This same value of t is then applied to the implicit model for all other Poisson's ratios. The model closely agrees with the elastic DD simulations for any value of ν for initially screw dislocations, as shown in Fig. 9(a). For initially edge dislocations, the model also accurately predicts β^{dis} for $\nu < 0.25$ (not shown) and only slightly exaggerates the magnitude β^{dis} at small applied stresses for $\nu > 0.25$, as shown in Fig. 9(b). This deviation may be a result of the finite core radius or discretization of the DD simulations.

The implicit model offers a significant improvement over the Hikata *et al.* and the power series solution. It confirms the importance of the orientation-dependence of line energy and the necessity of accurately calculating the area swept by a dislocation in calculating the ultrasonic nonlinearity parameter β. The elasticity DD simulations are sensitive to the orientation of the remote pinned segments, which cannot be captured by a line-tension model. However, initially screw dislocations are only marginally affected. Although the implicit solution for β^{dis} is lengthy, the solution process is conceptually simple and can be easily evaluated using a computer program.

VII. LENGTH DEPENDENCE OF β^{dis}

The proposed models can also be used to predict how β depends on the distance between the pinning points. The first-order and third-order terms of the power series solution in terms of σ in Eqs. (34) and (36) depend on $(L/b)^4$ and $(L/b)^6$ for a constant dislocation density, respectively. For stresses well below activation, β is predicted to depend on $(L/b)^4$ for screw and edge dislocations. This was verified using the implicit model for the case of $\nu = 0.30$ and an applied shear of $\sigma/\mu = 3.7 \times 10^{-5}$. The $(L/b)^4$ scaling is clearly exhibited by screw dislocations for lengths well below the critical value for Frank–Read source activation, as illustrated in Fig. 10(a). β tends to infinity at lengths approaching the activation length. Figure 10(b) reveals this is also the case for edge dislocations, but the deviation from $(L/b)^4$ occurs at smaller lengths. The cusp in Fig. 10(b) is a result of β changing sign for edge dislocations; β is negative lengths smaller

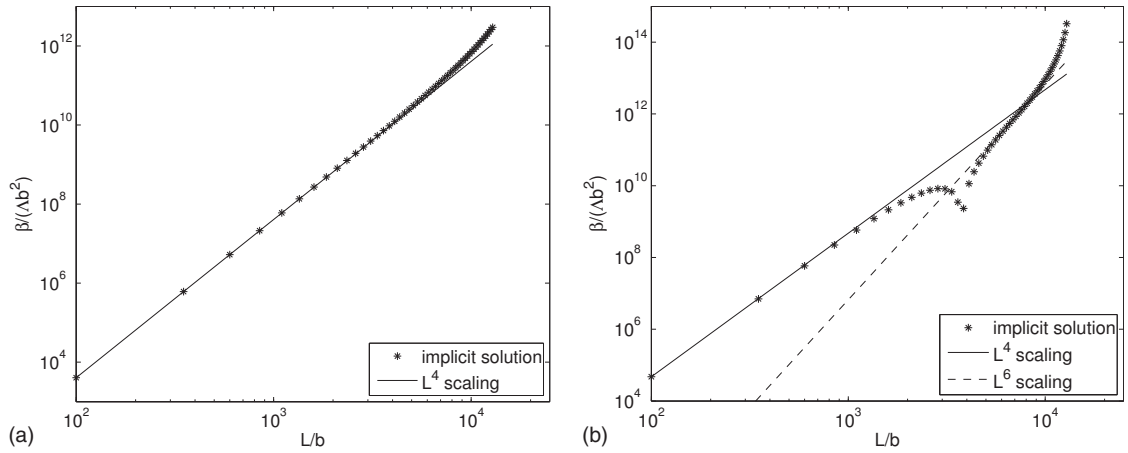

FIG. 10. Dependence of β on distance between pinning points ($\nu = 0.30$, $\sigma/\mu = 3.7 \times 10^{-5}$).

than the cusp, but the absolute value is taken for the logarithmic plot. Thus, β scales with $(L/b)^4$ for lengths with negative β values. However, the scaling is $(L/b)^6$ for positive values of β at lengths below the activation length. It should be noted that this behavior is only observed for edge dislocations where β changes sign; For $\nu < 0.25$ the results for edge dislocations qualitatively resemble those of screw in Fig. 10(a).

VIII. COMPARISON WITH PREVIOUS EXPERIMENTS

One of the main predictions of this work is that the dislocation contribution to acoustic nonlinearity, β^{dis}, can be negative. However, existing experiments only measure the amplitude of β, and provide no information on its sign. Assuming that the lattice contribution to acoustic nonlinearity, β^{lat}, is positive, a negative β^{dis} would lead to a decrease in the measured β with increasing stress. Unfortunately, there have been few experiments to measure how β depends on the applied stress, with the notable exception of the original papers by Hikata *et al.*[1,5]

For an unannealed sample, Hikata *et al.*[5] show a linear increase in β until attenuation becomes significant. Notably different behaviors are observed in their annealed samples, some of which have undergone plastic deformation before the acoustic measurement. All of these samples show an initial decrease in β, which is inconsistent with the constant line-tension model. Hikata *et al.* tried to explain this discrepancy in terms of internal stresses caused by the plastic deformation. This argument would lead to the prediction that β will increase with applied stress after the magnitude of the applied stress exceeds the internal stress. However, this is inconsistent with the data for the annealed sample that had not undergone any plastic deformation, as well as samples subjected up to 200 g/mm^2 stressing. In these cases, β decreased over the entire range of applied stress. In contrast, these results can be naturally explained in terms of the negative dislocation contributions to β.

The drastically different behavior after annealing indicates a significant change in dislocation microstructures. It is known that annealing reduces dislocation density and promotes the formation of stable dislocation structures.[22,23] An isolated dislocation monopole, considered by Hikata *et al.* and this work, is likely a better model for the microstructure after annealing. Hence, the observed decrease in β with stress in annealed fcc samples strongly supports the proposed orientation-dependent line energy model.

A dislocation monopole is only one of the proposed microstructures that contribute to acoustic nonlinearity. Another well-studied microstructure is a dislocation dipole.[3,6] It is predicted that a dislocation dipole has a positive contribution to β at zero applied stress, while the monopole contribution is zero. Therefore, it is reasonable to expect that the magnitude of contribution from dislocation dipoles to the experimentally measured β should be significantly larger than that from dislocation monopoles in materials under no applied stress. Hence, the decrease in β by irradiation[24] can be explained by the reduction in dipole contribution to beta, which is caused by the immobilization of dislocation dipoles.

Furthermore, care should be taken when comparing the predictions of monopole models with experimental measurements of fatigued samples.[3,25–27] Many of these experiments are performed on single crystals, whose microstructure is expected to be primarily composed of edge dislocation dipoles.[4] Therefore, dipole interactions should be the predominant dislocation mechanism that contributes to β, especially at zero applied stress.

IX. CONCLUSIONS

The model developed in this paper using an orientation-dependent line energy offers a significant improvement over the existing model using a constant line-tension. The agreement of the analytic solution of this model with DD simulations using elastic interactions verifies its accuracy and establishes the utility of DD simulations for studying β. DD simulations will allow for studying dislocation structures beyond the scope of analytical models and capture β as the structures evolve.

It is shown for the first time that a dislocation's contribution to β can be of opposite sign for a given stress state depending on the character angle of the dislocation, the distance between pinning points, and the Poisson's ratio of the material. The negative values of β can be quite significant for pure edge dislocations in materials with large Poisson's ratios. This is particularly important in fcc engineering metals, because edge dislocations are dominant in their fatigued microstructures. This allows for the cancellation of different contributions to β, such as that of the lattice or dislocation dipole motion.

Although the implicit solution is significantly more accurate in general, the power series solution has its own advantage. The simplicity of the power series solution allows one to easily predict when dislocations will have initially negative values of β, as shown in Fig. 7. Equations (34) and (36) also reveal that β is expected to scale with $(L/b)^4$ for stresses well below the activation stress. This suggests that β could be possibly be used as a measure of the length distribution of dislocation segments between pinning points.

ACKNOWLEDGMENTS

This work is funded by the Air Force Office of Scientific Research Grant No. FA9550-07-1-0464. W. D. Cash is supported by the Benchmark Stanford Graduate Fellowship. The authors would like to thank D. M. Barnett and W. D. Nix for their invaluable advice.

[1] A. Hikata, B. B. Chick, and C. Elbaum, Appl. Phys. Lett. **3**, 195(1963).
[2] J. Frouin, S. Sathish, and J. K. Na, Proc. SPIE **3993**, 60 (2000).
[3] J. H. Cantrell and W. T. Yost, Int. J. Fatigue **23**, 487 (2001).
[4] S. Suresh, *Fatigue of Materials* (Cambridge University Press, Cambridge, United Kingdom, 1998).
[5] A. Hikata, B. B. Chick, and C. Elbaum, J. Appl. Phys. **36**, 229(1965).
[6] J. H. Cantrell, Proc. R. Soc. London, Ser. A **460**, 757 (2004).
[7] J. H. Cantrell, J. Appl. Phys. **105**, 043520 (2009).
[8] R. K. Oruganti, R. Sivaramanivas, T. N. Karthik, V. Kommareddy, B. Ramadurai, B. Ganesan, E. J. Nieters, M. F. Gigliotti, M. E. Keller, and M. T. Shyamsunder, Int. J. Fatigue **29**, 2032 (2007).
[9] V. V. Bulatov, L. L. Hsiung, M. Tang, A. Arsenlis, M. C. Bartelt, W. Cai, J. N. Florando, M. Hiratani, M. Rhee, G. Hommes, T. G. Pierce, and T. D. de la Rubia, Nature (London) **440**, 1174 (2006).

[10]C. Déprés, C. Robertson, and M. Fivel, Philos. Mag. **84**, 2257 (2004).
[11]G. DeWit and J. S. Koehler, Phys. Rev. **116**, 1121 (1959).
[12]A. Arsenlis, W. Cai, M. Tang, M. Rhee, T. Oppelstrup, G. Hommes, T. G. Pierce, and V. V. Bulatov, Modell. Simul. Mater. Sci. Eng. **15**, 553 (2007).
[13]L. Dupuy and M. C. Fivel, Acta Mater. **50**, 4873 (2002).
[14]J. H. Cantrell, in *Ultrasonic Nondestructive Evaluation*, edited by T. Kundu (CRC, Boca Raton, FL, 2004).
[15]The strains here are a result of the applied stress and should not be confused with the arbitrarily small displacements from the acoustic wave.
[16]This is done to avoid introducing an arbitrary density and because $\Lambda^{\mathrm{dis}}b^2$ is a common factor in the power series model derived in this paper.
[17]This assumption has been numerically verified, but the discussion is omitted here.
[18]It should be noted that by varying ν while holding μ constant in an elastically isotropic medium will cause the Young's modulus E of the material to change. This obviously cannot be accomplished in a physical experiment, but is done here to illustrate the problem.
[19]A. J. E. Foreman, Acta Metall. **3**, 322 (1955).
[20]This model could be used for an arbitrary dislocation, but calculating A will be more difficult.
[21]The solution to Eq. (42) and all subsequent steps of the derivation of this model are omitted to save space.
[22]P. B. Hirsch, R. W. Horne, and M. J. Whelan, Philos. Mag. **1**, 677 (1956).
[23]A. S. Keh and S. Weissmann, in *Electron Microscopy and Strength of Crystals*, edited by G. Thomas and J. Washburn (Wiley, New York, 1962).
[24]M. A. Breazeale and J. Ford, J. Appl. Phys. **36**, 3486 (1965).
[25]J. Frouin, S. Sathish, T. E. Matikas, and J. K. J. Na, Mater. Res. **14**, 1295 (1999).
[26]J. Y. Kim, L. J. Jacobs, J. Qu, and J. W. Littles, J. Acoust. Soc. Am. **120**, 1266 (2006).
[27]J. H. Cantrell, J. Appl. Phys. **100**, 063508 (2006).